THE ASTROPHYSICAL JOURNAL, 361:459–469, 1990 October 1

EXTENDED X-RAY EMISSION IN NEARBY SEYFERT GALAXIES

MARTIN ELVIS AND C. FASSNACHT
Harvard-Smithsonian Center for Astrophysics
A. S. WILSON
Astronomy Program, University of Maryland
AND
U. BRIEL
Max-Planck-Institut für Physik und Astrophysik
Received 1989 December 28; accepted 1990 March 28

ABSTRACT

Asymmetric extended X-ray emission has been discovered around two Seyfert nuclei (NGC 1566 and NGC 2992) using the *Einstein* HRI. Extended X-ray emission is also present in NGC 4151. The emission amounts to 15%–30% of the total HRI X-ray flux and extends over ~ 1 kpc. Such extended X-ray emission is presumably a common feature in Seyfert galaxies since it has been found in three out of five Seyferts with sufficiently good HRI data. This extended emission is almost certainly associated with the nuclear activity, since the ratio of its X-ray flux to the B band flux from the same region is two orders of magnitude larger than is typical of early-type spirals.

We discuss various possible origins for this emission, including thermal bremsstrahlung, synchrotron radiation, inverse Compton scattering, and electron-scattered nuclear radiation. The present data, while favoring thermal models, are unable to discriminate between them definitively. If the extended X-ray emission is from hot gas, then this gas has a pressure comparable to that required for confinement of both the emission-line clouds in the extended narrow line region and the extended radio sources.

Subject headings: galaxies: interstellar matter — galaxies: Seyfert — galaxies: X-rays — radiation mechanisms

I. INTRODUCTION

Although signs of nonstellar activity away from the pointlike nuclei of Seyfert galaxies are commonly found in radio and optical images (Wilson and Heckman 1985), only one case of extended X-ray emission has so far been reported—in the famous Seyfert NGC 4151 (Elvis, Briel, and Henry 1983, hereafter EBH). The cause of this X-ray emission is not known, and several rival possibilities exist, including both thermal and nonthermal emission processes as well as electron scattered nuclear radiation. Other cases of extended X-ray emission might allow these possibilities to be tested.

There are several *Einstein* HRI observations of Seyfert galaxies that have not until now been carefully searched for extended emission. The HRI and mirror assembly provide a spatial resolution of $\sim 4''$ (FWHM) over the central 25′ of the *Einstein* focal plane for soft X-rays ($\sim$0.1–3 keV: Giacconi *et al.* 1979; Henry *et al.* 1977). Since most of the Seyferts in the HRI observations lie between 20 and 100 Mpc away (for $H_0 = 50$ km s^{-1} Mpc^{-1}, which we shall use throughout this paper), this resolution allows us to look for structures on a scale of ~ 1 kpc, similar to those seen in the radio and optical bands. We have thus systematically reexamined all the *Einstein* HRI data on Seyferts to search for extended X-ray emission.

II. OBSERVATIONS

We examined the reprocessed images of all the 20 observations of Seyfert galaxies made with the *Einstein* HRI (Seward and Martenis 1986). Out of these, six galaxies had observations with sufficient counts to search for a weak excess around the nucleus: NGC 4151 (two observations), NGC 1566, NGC 2992, NGC 7469, NGC 5548, and 3C 120. Details of the observations are given in Table 1A.

A comparison sample of sources known to be pointlike, from their variability, was treated in a manner identical to the Seyferts. This comparison sample allows us to determine the significance of any extent, since systematic errors (due, for example, to spacecraft attitude determination errors) may cause departures from simple counting statistics. We chose point sources that had count rates similar to those of the Seyferts in order to make the comparison as close as possible. It was surprisingly difficult to find such sources among the HRI observations. The 10 observations used are listed in Table 1B.

To guard against including data during times when the spacecraft attitude determination ("aspect") was poorly measured, we selected our data carefully. (Because the HRI records every incoming photon, unsteady motions of the satellite can be corrected for post facto with an aspect solution derived from the star trackers. Event positions are digitized in 0".5 pixels.) We used only "LOCKED" data, i.e., data that came from the HRI when the star trackers were actively tracking stars. "LOCKED" data give the best aspect solution (Harris, Stern, and Biretta 1990). Data that were taken when the trackers were scanning for guide stars ("MAPMODE"), which typically gives poorer aspect solutions (Harris, Stern and Biretta 1990), were rejected. Finally, one sequence number (6389) contained two observations 6 months apart. The source locations from the two halves were obviously offset from one another so we used only the longer of the two.

III. SEARCH FOR EXTENT

a) Location of Centroid

In order to find the center of the point source, we followed the procedure used in EBH: the counts within a 5 pixel (2".5) radius circle were determined at different locations centered

TABLE 1

Einstein HRI OBSERVATIONS

Object	Sequence Number	Date	Exposure Time (s)	Counts[a]	D(Mpc)[b]	T[c]
		A. Seyfert Galaxies				
NGC 1566	7112	1979 Dec 31	16697	1752	30	4
3C 120	6389	1981 Feb 14[d]	8322	790	200	...
NGC 2992	441	1978 Nov 22	10128	757	46	1
NGC 4151	6395	1980 May 20	9622	587	20	2
	340	1979 May 31	10189	506	...	...
NGC 5548	6397	1980 Jun 29	14705	4307	100	0
NGC 7469	10218	1981 Jan 6	12886	2628	84	1
		B. Comparison Sources				
3C 273	569	1978 Dec 14	96041	74558	...	...
Terzan 2	680	1979 Mar 5	2281	586	...	...
MXB 1905+00	3156	1979 Aug 30	3645	382	...	...
NGC 7078 (1)	4879	1979 Nov 19	960	773	...	...
(2)	4880	1979 Nov 19	1441	780	...	...
(3)	4881	1979 Nov 19	1341	1095	...	...
(4)	4882	1979 Nov 19	1232	1202	...	...
EX Hya	3505	1979 Jan 14	7442	3205	...	...
AM Her	3704	1979 Feb 22	1702	6908	...	...
PSR 0656+14M	9266	1981 Mar 29	4729	1309	...	...

[a] Counts = observed number of counts within a 10″ radius circle (no background subtracted).
[b] Palumbo *et al.* 1983, assuming $H_0 = 50 \text{ km s}^{-1} \text{ Mpc}^{-1}$.
[c] Morphological type, T, from de Vaucouleurs, de Vaucouleurs, and Corwin 1976.
[d] This sequence number contained two separate observations 6 months apart. Only the latter section was used in this paper (see text). The other, shorter, observation was on 1980 Aug 18.

near the peak. The circle was chosen to be this small to ensure that the nuclear point source dominates over any extended emission that may be present. Since each of these Seyferts is known to vary by a factor of at least 2 in hard X-rays (2–10 keV: NGC 4151, Lawrence 1980; 3C 120, Halpern 1985; NGC 2992 and NGC 7469, Marshall, Warwick, and Pounds 1981; NGC 5548, Branduardi-Raymont 1986; NGC 1566, Halpern 1982), we can be confident that the bulk of their X-rays come from regions too small to resolve with the HRI. The 2″.5 circle was divided into four quadrants along east-west and north-south lines, and at each point on the grid we compared the number of counts in each quadrant. The grid spacing is in integer pixels of 0″.5. Since this is ∼10% of the HRI FWHM, it is sufficiently fine so as not to introduce digitization asymmetries. It is also matched to the centroiding ability of the ∼100–400 photons in the central circle. The central point source position is then given by the location which best approaches equal counts in each quadrant, as determined by a χ^2 test.

For almost all of the galaxies, a clear minimum for χ^2 was found (Table 2A). The detector pixel locations are listed in Table 2. In all cases, the location indicated was within a few arcsec of the accurately measured optical position for the galaxy (Table 3A), consistent with the absolute aspect accuracy of the *Einstein* satellite. The similar offsets obtained for the comparison sample (Table 3B) confirm that these residual offsets are due to the limitations of the spacecraft aspect system.

Any observations for which we cannot clearly define a center, i.e. which had more than 3 pixels with values of χ^2 within 2.3 of $\chi^2_{\rm min}$ (68% confidence limit; Avni 1976), cannot be used reliably in our search, although this "problem" might itself be an indicator of structure. Only one observation, the earlier of the two NGC 4151 observations (sequence number 340), was removed because of this criterion.

Finally, we used only observations for which the minimum value for χ^2 in the central circle was consistent with symmetry (i.e., less than 10). Larger values of $\chi^2_{\rm min}$ might indicate small-scale structure in the Seyferts. However, since the comparison sample has a similar fraction of high χ^2 observations (Table 2B), they more probably indicate a poor satellite aspect solution. We thus prefer to be cautious and so eliminated NGC 5548 from the list of Seyfert galaxies, as well as three of the comparison point sources.

b) Search for Asymmetric Extent

We then made a search for *asymmetric* extended emission in the remaining Seyfert galaxies and in the comparison sample. This search will not find symmetric extended components. Such components are much more difficult to find since they require an accurate knowledge of the point-spread function, its energy dependence, and the spectrum of the X-ray source.

For the observations that survived the selection process, we placed a second, 10″ radius, circle centered at the detector centroid of the point source. Keeping the quadrant divisions along north-south and east-west lines, we looked for asymmetries in the counts in the annuli between 2″.5 and 10″ using a χ^2 test. Table 2 gives the resulting values of χ^2 for both the Seyferts and the comparison sample. The test, based solely on Poisson counting statistics, indicated that three of the Seyferts, NGC 4151, NGC 1566, and NGC 2992, had asymmetry, while the remaining two, NGC 7469 and 3C 120, were well fitted by a uniform distribution of counts (Table 2). We note that although the *Einstein* HRI point-spread function puts ∼40% of the emission from the central point nuclear source into this annulus, it has a 16-fold azimuthal symmetry and thus does not disturb the symmetry of counts in the outer annulus.

Systematic effects, most obviously from residual aspect errors, could create spurious asymmetries however. The true significance to assign to the χ^2 is best measured by comparison

TABLE 2

CENTROID PARAMETERS AND TEST FOR ASYMMETRIC EXTENDED EMISSION

Object	Sequence Number	Center (pixels) Y	Z	$\chi^2(2.5)$[a]	N[b]	$\chi^2(10)$[a]
A. Seyfert Galaxies						
NGC 1566	7112	2008	1987	1.9	1	302.1
3C 120	6389	2040	2054	6.2	1	5.8
NGC 2992	441	1530	2021	4.5	2	11.0
NGC 4151	6395	2028	2044	0.15	1	31.2
	340	2025	2024	1.9	7	...
NGC 5548	6397	2056	2046	21.1	1	...
NGC 7469	10218	2039	2051	2.3	1	4.1
B. Comparison Sources						
3C 273	569	2047	2048	128.1	1	...
Terzan 2	680	1991	2127	4.4	1	7.9
MXB 1905+00	3156	2089	2085	4.0	2	2.3
NGC 7078 (1)	4879	1564	2523	2.2	3	3.2
(2)	4880	2526	1567	3.1	3	1.3
(3)	4881	1566	1566	3.3	1	3.7
(4)	4882	2526	2524	3.7	1	4.1
EX Hya	3505	2510	2009	14.0	1	...
AM Her	3704	2052	2044	10.7	1	...
PSR 0656+14M	9266	2018	2114	2.5	1	2.1

[a] χ^2 value for annuli between inner radius 0″ and outer radius 2″.5 (2″.5) and between inner radius 2″.5 and outer radius 10″ (10″) centered on centroid (Y, Z). Observations with $\chi^2_{min} > 10$ and/or $N > 3$ were not used (see § IIIa).

[b] N = number of pixels with $\chi^2 < (\chi^2_{min} + 2.3)$ 68% confidence interval for two free parameters (Avni 1976).

with the point source sample. Figure 1 compares the distribution of χ^2 in the outer annuli from the Seyferts with that of the comparison point source sample. The comparison sample shows no significant high χ^2 tail above the value of 3 expected. This strengthens our confidence in the reality of the asymmetrically extended emission in the three Seyferts based on the χ^2 test. NGC 4151 and NGC 1566 easily exceed any χ^2 in the point source sample, and NGC 2992 also has a χ^2 above any χ^2 in the point source sample, although by a smaller amount. We conclude that NGC 4151, NGC 1566, and NGC 2992 have extended X-ray emission.

We can determine upper limits to any asymmetric extended emission for the other two Seyferts, 3C 120 and NGC 7469. Any asymmetry must cause a $\chi^2 > 11$ for us to find that the

TABLE 3

COMPARISON OF X-RAY AND OPTICAL POSITIONS[a]

Object	Sequence Number	X-Ray R.A.	X-Ray Decl.	Optical R.A.	Optical Decl.	References[b]	Δ[c]
A. Seyfert Galaxies							
	7112	$04^h18^m53^s.28$	−55°03′22″.5	$04^h18^m53^s.3$	−55°03′23″.0	1	0″.5
	6389	04 30 31.72	05 14 58.2	04 30 31.61	05 14 59.8	2	1.6
	441	09 43 17.76	−14 05 46.5	09 43 17.53	−14 05 44.8	3	3.8
	6395	12 08 01.21	39 41 03.5	12 08 1.06	39 41 01.8	2	1.7
	10218	23 00 44.71	08 36 16.2	23 00 44.43	08 36 16.1	2	0.1
B. Comparison Sources							
	569	12 26 33.18	02 19 43.2	12 26 33.24	02 19 43.2	3	1.0
	680	17 24 20.02	−30 45 39.6	17 24 19.8	−30 45 40.3	5	0.9
	3165	19 05 53.43	00 05 18.2	19 05 54	00 05 20	4	...
	4879	21 27 33.18	11 56 51.1	21 27 33.0	11 56 49.6	5	2.6
	4880	21 27 33.21	11 56 49.1	21 27 33.0	11 56 49.6		2.0
	4881	21 27 33.11	11 56 49.6	21 27 33.0	11 56 49.6		1.7
	4882	21 27 33.21	11 56 50.6	21 27 33.0	11 56 49.6		3.1
	3505	12 49 42.33	−28 58 40.4	12 49 42.9	−28 58 40	5	7.5
	3704	18 14 58.26	49 50 56.4	18 14 59	49 50 58.6	5	3.6
	9266	06 56 57.94	14 18 30.69	06 56 57	14 15	6	...

[a] All positions are 1950.0.

[b] REFERENCES FOR OPTICAL POSITIONS.—(1) Wilson and Meurs 1978; (2) Clements 1981; (3) Clements 1983; (4) Remillard 1988; (5) Bradt and McClintock 1983; (6) *radio position*, Manchester and Taylor 1981, uncertain by 5′.

[c] Δ = offset between optical and X-ray positions.

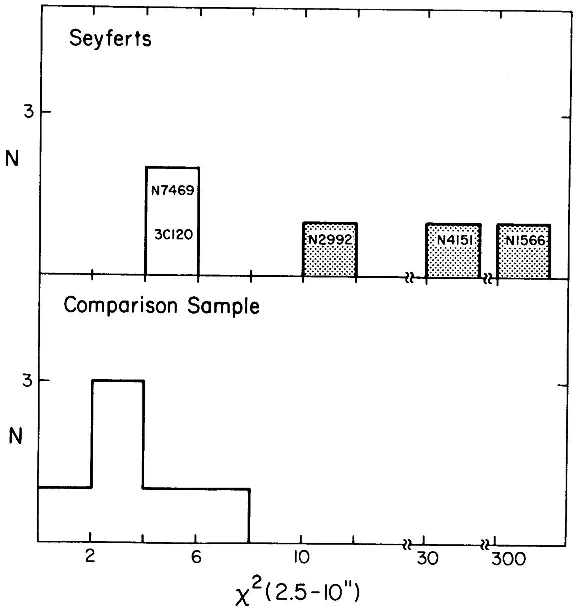

FIG. 1.—χ^2 distributions for the Seyferts and the comparison point source sample. χ^2 values are for 2".5–10" annuli divided into four quadrants (as in Fig. 2).

source has asymmetric extent (Fig. 2). 3C 120 and NGC 7469 would require 20 and 33 more counts, respectively, in the quadrant with the highest number of counts in order to show asymmetric extent at this level.

c) *Structure of NGC 1566 on an Arcminute Scale*

Because the asymmetry in NGC 1566 is so pronounced (Fig. 2) and the number of counts is large, we made a map to search for large scale features. Figure 3 shows the *Einstein* HRI map of NGC 1566 smoothed with a 5" Gaussian. On this scale the small scale asymmetry in the inner 20" diameter region cannot be seen. On a 1' scale, the *Einstein* HRI image shows clear evidence for extent along roughly the same axis (p.a. ~ 130°) as on the smaller scale, although with the greater extension being in the opposite (SE) qudrant.

Radial profiles in 10" bins from 10" to 120" (with the background, determined from a 120"–180" annulus, subtracted out) show a clear excess to the NW in the first 10"–20" bin but no significant excess beyond that. To the SE, the same profiles show extensions at the 1 σ level in each bin out to 60"–70". The outer SE excess has a significance of 3 σ when determined from these profiles.

IV. CHARACTERISTICS OF ASYMMETRIC EXTENT

a) *Position Angle*

We can locate the position angle of the extended emission by rotating the "pie" diagrams of Figure 2 in steps and noting where the asymmetry is maximized.

The pattern in the point spread function produced by the 16 equally spaced mirror supports repeats at 22°.5 intervals, so rotation steps of this size were used. In this way all the position angles used are symmetric with respect to this structure in the point response function. This gives a check on extent along the N-S, E-W divisions for NGC 7469 and 3C 120 and defines the position angle of the extent somewhat better in the other three objects. Figure 2 shows the distribution of counts so found for these three Seyferts with high χ^2. For NGC 7469, no position angle gave a high χ^2. For 3C 120 χ^2 rises to 12 at p.a. 67°.5 and at p.a. 22°.5. This peculiar behavior suggests some structure, but on a scale that is smaller than the HRI point spread function.

Figure 4 shows χ^2 versus the position angle of the quadrant with the most counts. For all three cases, a maximum is defined (Table 4), although for NGC 1566 and NGC 4151 it is not strongly peaked. A wide peak suggests that the X-ray emission is not well contained within the quadrant. For NGC 1566 the χ^2 test returns a very high value (> 100) for all position angles tested, suggesting that the excess emission in NGC 1566 is both very strong and extended over ~90°. The large scale emission (Fig. 3) strengthens this conclusion.

b) *Radial Profile*

The radial extent of the asymmetric extended emission was investigated by subtracting the mean of the other three quadrants from the high count quadrant in successive 2".5 radial steps. The counts in each step were then converted to surface brightness, and their radial profiles are shown in Figure 5. (Note that the centroiding procedure of § III*a* guarantees that the 0"–2".5 bin has essentially zero flux.) All three galaxies show

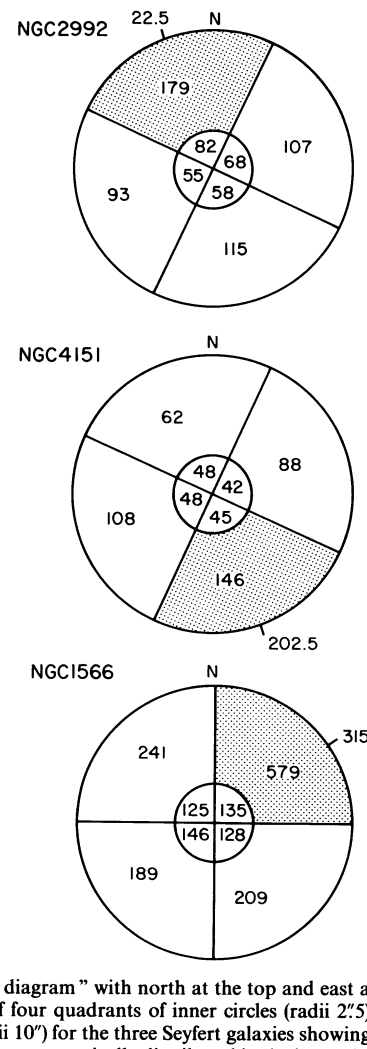

FIG. 2.—"Pie diagram" with north at the top and east at the left, showing counts in each of four quadrants of inner circles (radii 2".5) and surrounding annuli (outer radii 10") for the three Seyfert galaxies showing asymmetry. Note that the counts are symmetrically distributed in the inner circle. The quadrants of the annuli with excess counts are shaded. The best-fit position angle of the excess is shown.

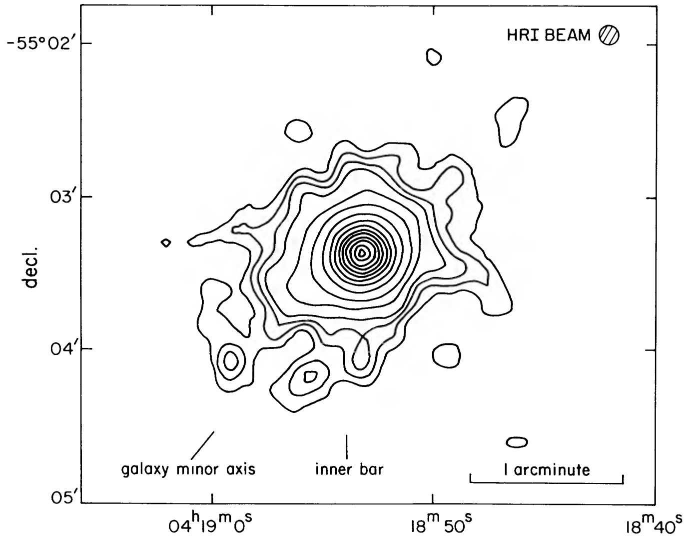

FIG. 3.—Contour map of the NGC 1566 HRI image. The image has been smoothed with a 5″ Gaussian filter, similar in size to the HRI point response function. The position angles of the inner bar and the galaxy minor axis (determined from the outer isophotes) are shown. Contours are in counts arcsec^{-2} s^{-1} at the following values: 3.0, 3.8, 4.8, 5.9, 8.6 14.4, 34, 74, 125, 186, 256, 334, 419, 511, 570.

a significant excess from 2″.5 out to at least the 7″.5–10″ bin (Table 4). The X-ray surface brightness declines rapidly with radius for NGC 1566, but more slowly for NGC 2992 and NGC 4151.

c) *Count Rate*

We have estimated the total number of counts in the excess region. This requires several steps. To determine the directly observed count rate for the excess, we subtracted the mean of the other three quadrants from the high quadrant. This directly observed count rate needs to be increased to correct for the loss of counts due to the point-spread function of the HRI. A 4″ radius circle has almost the same area as a quarter of an annulus with inner and outer radii of 2″.5 and 10″, respectively. The HRI PRF within a 4″ radius includes only 40% of the counts from a point source (Harris 1984), so we increased the excess counts by a factor 2.5 as an approximate correction for this effect (Table 4). If the off-nuclear emission is not pointlike but extended by even a few arcseconds (as is suggested by the position angle and radial profile plots; Figs. 4 and 5), then even more photons will be scattered out of the high quadrant and this correction factor should be larger. We would then have *underestimated* the extended X-ray fluxes. On the other hand, it is also possible that there is extended emission outside of the high quadrant photons from such emission would be scattered into the high quadrant, leading to an *overestimate* of flux. Unfortunately, the data are inadequate to estimate these corrections, so we are forced to ignore them in the following analysis.

To determine the total count rate from the source (i.e., nucleus plus extended region), we integrated the counts over a circle of large radius (40″ = 80 pixel). This size circle contains 85% of the total emitted counts from a point source (Harris 1984), so the observed count rate was corrected by a factor 1.18. With a circle this large, the fact that the extended emis-

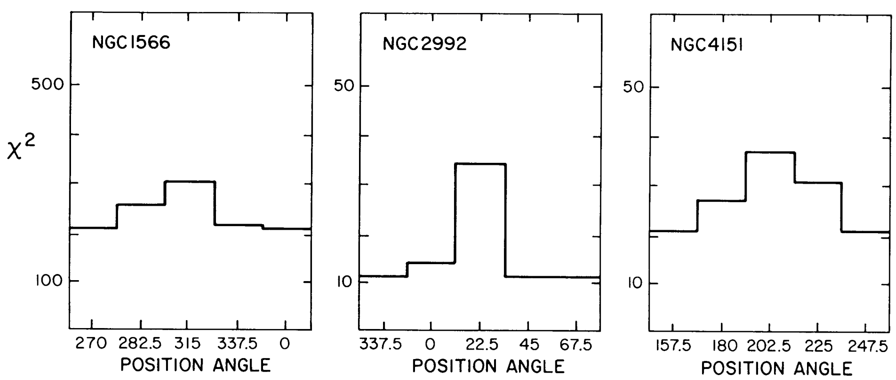

FIG. 4.—Variation of χ^2 (defined as in Fig. 2) with position angle of pie diagram quadrants. The peak χ^2 indicates the position angle of extended emission.

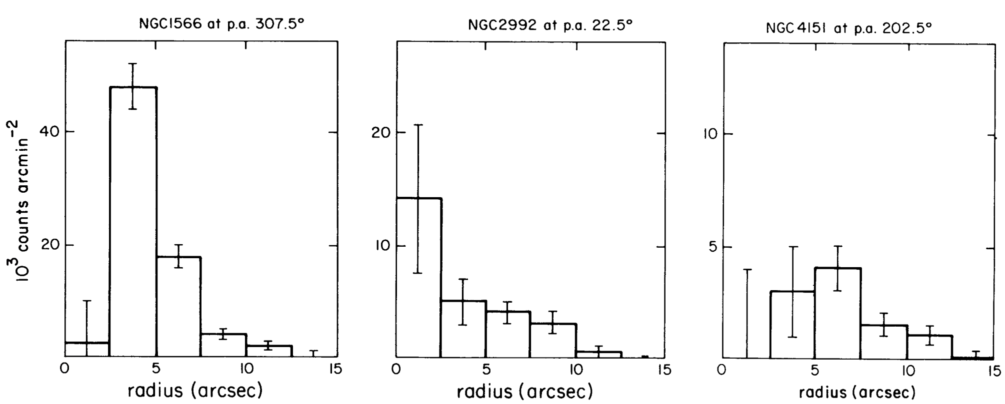

FIG. 5.—Radial profiles of X-ray surface brightness in the quadrants with the maximum counts. The mean surface brightness of the other three quadrants has been subtracted.

TABLE 4

PARAMETERS OF ASYMMETRIC EXTENDED X-RAY EMISSION

Seyfert	Count rate[a]	Per cent of Total	r_{max}	r_{max}(kpc)	X-ray p.a.	Radio p.a.	Emission Line p.a. (°)	Galaxy Major Axis p.a.
NGC 1566	54.8 ± 3.1	33.8	7″.5	1.1	338°	...	...	50°[b]
NGC 2992	18.3 ± 1.7	14.8	10.0	2.2	23	160°[c], 130°[d]	...	25[e]
NGC 4151	15.6 ± 1.6	15.4	7.5	0.73	203	257[f], 237[g]	231[h]	130[i], 26[j]
NGC 1566	8.7 ± 3.0	7.0	20 (NW)	2.9	310	...	...	...
(larger region)	...	...	60 (SE)	8.8	130	...	...	...
3C 120	< 5.7	< 3.5	...	...	...	...	...	...
NGC 7469	< 6.4	< 2.1	...	...	...	...	...	...

[a] 10^{-3} HRI counts s^{-1}.
[b] Major axis of faint outer arms (de Vaucouleurs 1973).
[c] On ≃8″ scale (Ulvestad and Wilson 1984).
[d] On ≃25″ scale (Hummel *et al.* 1983).
[e] On a few × 10″ scale (Durret and Bergeron 1987; Colina *et al.* 1987).
[f] On ≃4″ scale (Wilson and Ulvestad 1982; Johnston *et al.* 1982).
[g] On ≃20 mas scale (Harrison *et al.* 1986).
[h] On ≃15″ scale (Heckman and Balick 1983; Pérez- Fournon and Wilson 1990).
[i] Arcmin scale bar (Simkin 1975).
[j] Outer disk (Simkin 1975).

sion is offset by a few arcseconds from the nucleus is not significant in determining the combined number of counts from both regions.

For the arcminute-scale structure in NGC 1566 (Fig. 3) we were interested in the X-ray count rate in annulus with inner radius of 10″ (thus excluding the inner extended region) and outer radius of 1′. Within this annulus, there is an excess of 545 counts above a background of 178 counts (determined from the annulus between radii 120″ and 180″ with the same center). In the same region, 419 counts are expected through scattering from the nuclear source, leaving an excess of 126 counts due to extended emission. The correction factor to apply to these counts is uncertain because of the complex distribution of flux. A factor of 1.15 (corresponding to a radius around a point source of 45″) is a reasonable estimate. This leads to a corrected count rate of 8.7 ct ks^{-1}.

For NGC 4151 and NGC 2992 the asymmetric X-ray excesses between 2″.5 and 10″ represent ∼15% of the total count rate, while that of NGC 1566 on the same angular scale accounts for 34% of the total galaxy count rate (Table 5). The larger region of extended X-ray emission in NGC 1566 provides another 7%.

d) Fluxes and Luminosities

The fluxes and luminosities of the extended X-ray emissions may be estimated from the corrected count rates, for assumed spectral forms. We computed these values assuming simple thermal bremsstrahlung emission at two temperatures representing the extremes to which the HRI is sensitive, namely $kT = 0.1$ keV and $kT = 3.0$ keV. Conversion factors were derived as in the *Einstein* Revised Users' Manual (Harris 1984). These factors allow for photoelectric absorption by gas in our

TABLE 5

FLUXES AND LUMINOSITIES OF ASYMMETRIC EXTENDED REGIONS

Seyfert	F_X[a,b]	L_X[a,c]	f_B[d]	log (f_X/f_B)[e]	$(U-B)$[f]	N_H(Gal)
NGC 1566	6.9, 5.4	7.5, 5.9	6.7	−4.01	0.28[g]	1.7[h]
NGC 2992	11.6, 2.7	30, 6.8	2.1	−3.81	0.56[i]	5.6[j]
NGC 4151	2.5, 1.7	1.2, 0.80	2.8	−4.13	0.34[k]	2.1[l]
NGC 1566 .... (larger region)	1.1, 0.86	1.20, 0.94	150	−6.16	−0.01[g]	
3C 120	<15.9, 1.18	<768, 57				12.3[i]
NGC 7469	<3.24, 0.89	<28, 7.6				4.8[i]

[a] For optically thin bremsstrahlung with $kT = 0.1$ keV (first value) and $kT = 3.0$ keV (second value), over the energy range 0.1–3.5 keV, corrected for absorption assuming the Galactic value of N_H.
[b] 10^{-12} ergs cm^{-2} s^{-1}.
[c] 10^{41} ergs s^{-1}.
[d] 10^{-26} ergs cm^{-2} s^{-1} Hz^{-1}, converted from B magnitudes.
[e] As in Fabbiano and Trinchieri 1985. f_X is the monochromatic X-ray flux density in ergs cm^{-2} s^{-1} Hz^{-1} at 2 keV and has been calculated assuming optically thin bremsstrahlung at $kT = 3.0$ keV.
[f] $(U-B)$ color in 2″.5–10″ radius annulus, except for the larger region of NGC 1566 where it is for a 10″–60″ radius annulus.
[g] Longo and de Vaucouleurs 1983.
[h] 10^{20} atoms cm^{-2}; Heiles and Cleary 1979.
[i] Neizvestry 1986.
[j] 10^{20} atoms cm^{-2}; Elvis, Lockman, and Wilkes 1989.
[k] McAlary *et al.* 1983.
[l] 10^{20} atoms cm^{-2}; Stark *et al.* 1984.

Galaxy using the known Galactic N_H values (Table 5) and assuming solar abundances. The results are given in Table 5.

The upper limits on any asymmetrically extended emission in 3C 120 and NGC 7469 are 5.7 counts ks^{-1} and 6.4 counts ks^{-1}, respectively. The corrections for the PRF have been made to these count rates, as for the detected extended regions (Table 5).

V. DISCUSSION

We have discovered asymmetrically extended X-ray emission in two Seyfert galaxies, NGC 1566 and NGC 2992, adding to previously known extended emission in NGC 4151. This extended emission comprises 15%–35% of the total kilovolt emissions in these three galaxies. The upper limits on extended X-ray emission for the remaining two Seyferts in our sample are comparable both in luminosity and fraction of the total. Significant amounts of extended X-ray emission appear, therefore, to be a common phenomenon in Seyfert galaxies.

This emission provides us with a new means of studying the "extranuclear" activity (e.g., Meurs and Fosbury 1990) in AGN. The presence of X-ray emission away from the nucleus will certainly affect the interpretation of the soft X-ray spectra of AGN, at least at low luminosities.

What is the nature of this extended emission? There are several possibilities. EBH and Heckman and Balick (1983) suggested that hot gas, heated by shocks induced by outflowing "narrow emission-line region" (NLR) gas or by the radio jet, in the interstellar medium of the host galaxy might be responsible. A hot gas may also be in pressure balance with the emission line gas and/or the radio plasma. A different possibility, made more plausible by the discovery of the "hidden Seyfert 1" spectrum of NGC 1068 (Antonnuci and Miller 1985), is that the X-rays originate in the nucleus but are then scattered into our line of sight by free electrons (Fabian 1977).

First, however, we must establish whether this is, in fact, abnormal emission associated with the active nucleus, or is simply normal galaxy X-ray emission from compact binaries and SNR. Since the work of EBH our knowledge of the X-ray properties of normal galaxies has advanced considerably (Fabbiano 1989), so that we can now compare the extended emission in Seyferts with that of normal galaxies of similar Hubble type.

a) Comparison with Normal Galaxies

The distribution of X-ray (2 keV) to optical (*B* band) monochromatic flux density ratios (f_x/f_B) for early-type spiral galaxies is well determined (Fig. 6; Fabbiano and Trinchieri 1985). Since the radial distribution of the X-rays and the *B* band light are also similar (Fabbiano 1989), we can compare the ratios of the extended X-ray emission to optical fluxes from the same regions for the Seyferts with those of normal galaxies to see if the X-ray excesses are typical of normal galaxies (Fabbiano and Trinchieri 1985). The host galaxies of these three Seyfert nuclei are all early type ($0 \leq T \leq 4$; Table 1).

This comparison is shown in Figure 6. To determine the optical flux from the regions with extended X-ray emission, we used the *B* band aperture photometry from the catalog of Longo and de Vaucouleurs (1983), subtracting the flux from within a 2″.5 radius from that within a 10″ radius and dividing the result by 4 to estimate the flux from a single quadrant. Using X-ray fluxes, f_X, derived from Table 5 gives us log (f_x/f_B) values of -4.13 to -3.81 (Table 5) for the Seyferts,

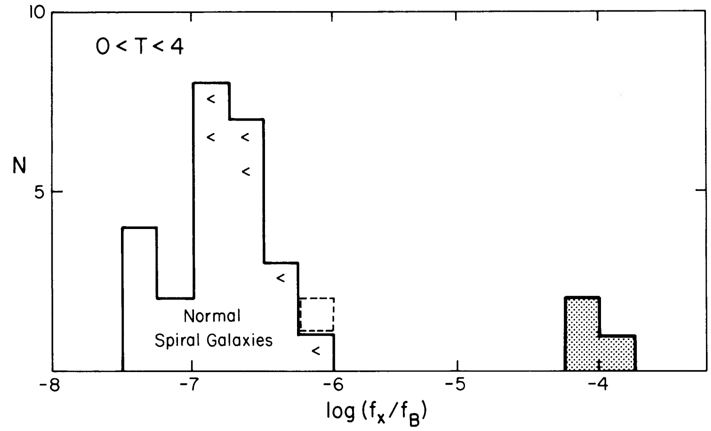

FIG. 6.—Comparison of the X-ray–to–optical monochromatic flux ratios (log f_X/f_B) for the extended X-ray emission of the Seyfert galaxies with those of normal galaxies of the same morphological type ($0 < T < 4$). The shaded boxes represent the extended inner regions of NGC 1566, NGC 2992, and NGC 4151, while the dashed box represents the outer region of NGC 1566.

compared with a maximum of -6.0 for the normal galaxies. Clearly the inner extended X-ray regions in the Seyferts are much too X-ray bright (i.e., large f_x/f_B) to be explained by processes common in normal galaxies. Since the luminosities of the extended emission (Table 5) are ~100–1000 times higher than those of the most luminous individual X-ray sources seen in normal galaxies, the enhanced log (f_x/f_B) values cannot be caused by a chance arrangement of a few bright sources in these small, kiloparsec-scale, regions. The extended X-ray emission is thus surely related to the presence of an active nucleus.

A different result is found for the large scale (~arcminute) structure seen in NGC 1566. The optical flux for this extended X-ray region was again derived from the photometric *B* magnitudes given in Longo and de Vaucouleurs (1983). For this annulus log (f_x/f_B) = -6.12. This value is at the extreme high end of the distribution in Fabbiano and Trinchieri (1985), but it is not clearly in excess of the normal galaxy range. This arcminute-scale X-ray emission may reflect unusually large numbers of X-ray binaries in the inner disk of NGC 1566 rather than emission related to the active nucleus. At least 40, and more probably 400–4000, X-ray binaries would be needed. The alignment with the inner region of extended X-ray emission does, however, suggest some connection between the nucleus and this larger region.

b) Estimation of Physical Parameters for the Case of Hot Gas

If we assume that the source of the asymmetric extended X-ray emission is diffuse hot gas, then we can estimate some of its physical parameters. Using the standard formulae for optically thin bremsstrahlung (Tucker 1975), and approximating the emitting volume as a uniform sphere of radius 4″, we can calculate the electron densities in the inner regions. The correct volume to take for the outer regions of NGC 1566 is less obvious. We have used a sphere of 30″ radius, which covers an area equivalent to one quadrant of the 10″–60″ annulus. We performed this calculation for one temperature (kT = 3.0 keV), but there are simple scalings to other values for $kT > 0.1$ keV (see Table 6). In all cases the values of n_e that we calculated imply an optical depth $\ll 1$, confirming that the gas is optically thin. Once the electron density is known, the approximate

TABLE 6

DERIVED PHYSICAL PARAMETERS[a]

Seyfert	Density n_e(cm^{-3})	Mass $M(10^6\,M_\odot)$	Cooling Time $t_{cool}(10^6$ yr)	Pressure $n_e T$[b]
NGC 1566[c]	1.4	30.8	24	49
NGC 2992[c]	1.6	112	22	55
NGC 4151[c]	1.1	6.5	32	37
NGC 1566[d] .... (larger region)	0.029	247	1179	1.0

[a] For optically thin bremsstrahlung from a uniform sphere, for $kT = 3.0$ keV. n_e and M scale as $T^{1/4}$, while t_{cool} and pressure ($n_e T$) scale as $T^{3/4}$.

[b] 10^6 cm^{-3} K.

[c] Taking a uniform sphere of 4″ radius as equivalent to the volume of emission (see text).

[d] Taking a uniform sphere of 30″ radius as equivalent to the volume of emission (see text).

mass and pressure of the regions can be found. Finally, we can calculate the cooling time of the gas. All these results are summarized in Table 6. Because of the uncertainties in the geometry and filling factor (assumed to be unity) and the possibility of departures from uniform density, the figures in Table 6 should be considered merely illustrative. They also ignore the possible presence of symmetric extended X-ray emission, and in this sense the densities are lower limits.

c) Comparison with Optical and Radio Structures

Although our X-ray data are crude, we can compare the position angles of the extended X-ray emission with those of the radio and optical emission-line structures on similar, few arcsecond, scales (Table 4).

In NGC 4151, EBH noted that the [O III] structure (Heckman and Balick 1983; see also Pérez-Fournon and Wilson 1990) had a similar p.a. to the X-rays and that both were displaced from that of the arcsec scale radio source (Table 4). Our estimate of the X-ray p.a. is displaced by one bin (22°.5) from that found by EBH and is now significantly different from that of the radio and optical emission-line structures. This change of p.a. reflects the uncertainties involved in using such low-resolution X-ray observations. The X-ray p.a. in NGC 4151 does align with the disk major axis, but the significance is doubtful given the almost face-on orientation of the galaxy.

The position angle of the X-ray source in NGC 2992 aligns well with the optical major axis of this highly inclined, dusty galaxy. There seems to be no clear connection with the "figure-of-eight"-shaped radio source on the 8″ scale (Ulvestad and Wilson 1984). [O III] λ 5007 emission extends over $\simeq 24''$ with a largely chaotic velocity field (Colina *et al.* 1987; A. S. Wilson and J. A. Baldwin, unpublished). Apart from indicating that the extended X-ray emission of NGC 2992 probably arises in the disk of the galaxy, our low-resolution observations provide no clear directions for modeling this emission.

No good resolution radio map of NGC 1566 has been published, due to its southern declination. Optically, de Vaucouleurs (1973) has provided isophotes, luminosity profiles and photometric parameters for the galaxy. The galaxy minor axis (130°) is similar to that of the inner X-ray extent. Pence, Taylor, and Atherton (1990) have recently mapped the [O III] velocity structure in the arcminute-scale inner disk.

d) Considerations for Emissions Mechanisms

Several emission mechanisms have already been proposed for the extended emission in NGC 4151 (EBH; Heckman and Balick 1983)—nonthermal, either direct synchrotron emission or inverse Compton; thermal emission from hot gas, either from a shock at the outflow/ISM boundary or as a emission-line cloud–confining medium; and integrated X-rays from binaries and SNRs generated in a nuclear starburst. To these we can add electron-scattered flux from the nuclear region. With three examples now in hand, we can reconsider each of these possibilities and note possible observational means for discriminating between them.

i) *Direct Synchrotron or Inverse Compton*

The radio jets in Cen A (Feigelson *et al.* 1981) and M87 (Schreier, Gorenstein, and Feigelson 1982) both show X-ray emission that is closely cospatial with the radio structure at a flux level that lies on reasonable, though uncertain, extrapolations of the radio-IR-optical spectrum. They are thus quite straightforwardly explained by synchrotron emission, although the short electron lifetimes involved require *in situ* acceleration. Another potentially important X-ray emission mechanism is inverse Compton scattering of the relativistic electrons in the radio jet. The lack of any agreement between the X-ray and radio position angles in the Seyferts (Table 4) argues against these processes. Higher resolution X-ray images could test whether such relativistic processes are important closer to the active nucleus.

ii) *Hot Gas*

Optically thin thermal emission from a plasma at 10^6–10^7 K is a plausible mechanism. Table 6 gave some relevant derived parameters assuming optically thin bremsstrahlung (see § V*b*). It is notable that the pressures derived are similar to those needed to confine the 10^4 K gas of the narrow emission-line regions at their densities of 10^{2-4} cm^{-3}. In particular, Penston *et al.* (1990) have recently measured the density and temperature in the optical extended ($\sim 15''$) narrow-line region of NGC 4151. The spatial scale of this region is very similar to that of the X-ray emission. They find $n_e = 160$ cm^{-3} and $T_e = 1.4 \times 10^4$ K, corresponding to a pressure $n_e T = 2.2 \times 10^6$ cm^{-3} K, which is very close to the pressure of the X-ray–emitting gas for $kT = 0.1$ (Table 6). If the hot gas is, indeed, the confining medium for the optical emission-line clouds, then its filling factor must be close to unity, and higher resolution X-ray maps should show a diffuse region over the whole extended narrow line region.

Emission-line cloud velocities of order 100–200 km s^{-1} would yield soft X-ray ($\sim 10^6$ K) temperatures if the velocities are thermalized in cloud-cloud or cloud-intercloud medium collisions. For NGC 4151, however, the line widths in the extended narrow line region are <40 km s^{-1} (Schulz 1988), too low to create significant X-ray emission. Closer to the nucleus, cloud velocities of the required magnitude do exist. Perhaps the hot gas is generated close ($\leq 4'' \simeq 400$ pc) to the nucleus and then expands in a wind to the several kpc scale.

Another process capable of generating hot gas is thermalization of outflow velocities at the ends of radio jets. Our data provide no evidence for this process, the radio jet in NGC 4151 being only 4″ long—much smaller than the extended X-ray emission—and in a different p.a. The X-ray and radio p.a.'s are also different in NGC 2992 (Table 4).

iii) *Starbursts*

Although the f_x/f_B ratios of these regions are far too large to explain with normal galaxy emission (Table 5; Fig. 6), some unusual starburst regions are seen to have several times larger

f_x/f_B ratios—up to log $f_x/f_B = -5.5$ (Fabbiano, Trinchieri, and MacDonald 1984). The emission is probably due mostly to large numbers of SNR and compact binaries (Fabbiano, Trinchieri, and MacDonald 1984). The $(U-B)$ color is a good predictor for this enhancement (Fabbiano, Trinchieri, and MacDonald 1984). The $(U-B)$ colors of these regions, again using aperture photometry from the literature, are given in Table 5. With the possible exception of the larger region in NGC 1566, the colors are in the range of those for normal galaxies ($\sim 0.5 < (U-B) < 0.2$) rather than those of starbursts ($\sim 0.1 < (U-B) < -0.5$). Thus although better color mapping of these regions should be carried out, there is currently no indication of starbursts. A starburst would probably be distinguishable by a two-component X-ray spectrum due to contributions from SNR (soft with many emission lines) and compact binaries (hard).

iv) *Electron-scattered Nuclear Flux*

An early report of extended X-ray emission in Cen A (Delvaille, Epstein, and Schnopper 1978) led to the suggestion that warm or hot plasma around the nucleus could electron scatter a reasonable fraction of the nuclear flux into our line of sight (Fabian 1977). The discovery of this effect in the polarized optical spectrum of NGC 1068 (Antonucci and Miller 1985) makes it worthwhile to reconsider this idea. The X-ray spectrum of the type 2 Seyfert galaxy NGC 1068 seems to be dominated by scattered flux (Elvis and Lawrence 1988; Koyama 1989). The fraction, f, of the observed luminosity in the scattered component is given by

$$f = \frac{F_{\rm scatterer}}{F_{\rm Earth}} \frac{\Omega_{\rm scatterer}}{4\pi} \tau_{\rm scatterer} ,$$

where $F_{\rm scatterer}$ and $F_{\rm Earth}$ are the fluxes of the nuclear X-ray source in the direction of the scattering medium and Earth, respectively; Ω is the solid angle in steradians subtended by the scattering regions as viewed from the nucleus; and τ is the electron scattering optical depth through the scatterer.

For NGC 4151 and NGC 2992 the intrinsic X-ray luminosity is larger than the total observed HRI luminosity because the *nuclear* source is heavily absorbed at HRI energies. For NGC 2992 the nuclear absorbing column density is ~ 1–2×10^{22} atoms cm^{-2} (see Maccacaro, Perola, and Elvis 1982 for data contemporaneous with the HRI observations, and Turner and Pounds 1989 for the latest high-quality measurements); for NGC 4151 the nuclear column density is complicated (Yaqoob, Warwick, and Pounds 1989) but is generally somewhat larger, ~ 5–15×10^{22} atoms cm^{-2}. Column densities of 1, 5 and 10×10^{22} atoms cm^{-2} will reduce the observed HRI nuclear luminosity by factors of 2.5, 6.3 and 10, respectively (Harris 1984, assuming a power law energy index of 0.5 appropriate to these objects; Turner and Pounds 1989). In the following we focus our discussion on NGC 4151, noting that similar arguments may apply to NGC 2992.

The *scattered* X-ray luminosity may also be reduced by the presence of photoelectrically absorbing columns of gas, both between the nucleus and the scattering medium and between the scattering medium and Earth. We have no way of estimating the column density between the nuclear X-ray source and the scattering medium. It could be comparable to that between the nuclear X-ray source and Earth, in which case $F_{\rm scatterer} \sim F_{\rm Earth}$, or it could be negligible, in which case $F_{\rm scatterer} \sim 10 F_{\rm Earth}$. We shall assume zero absorbing column density between the scattering medium and Earth, since the optical emission-line ratios obtained by Penston *et al.* for the extended narrow-line region in NGC 4151 imply that A_V is essentially zero.

$\Omega/4\pi$ can be constrained roughly since the opening half-angle for a cone is at least 45° since the χ^2 plot of Figure 4 is not sharply peaked and is probably not more than 60° in order for us to still observe asymmetry. (A better determination of this opening angle would be valuable.) This implies $0.25 < \Omega/4\pi < 0.15$, assuming conical symmetry with the arms in the plane of the sky. Since f is ~ 0.15, we find $0.06 < \tau < 0.10$ if $F_{\rm scatterer} \sim 10\ F_{\rm Earth}$, or $0.6 < \tau < 1$ if $F_{\rm scatterer} \sim F_{\rm Earth}$. These numbers imply a range in mean radial column density of $9 < N_{\rm H} < 150$ (in units of 10^{22} atoms cm^{-2}). In reality, radial density gradients and inhomogeneities are likely to be present.

This range in column density corresponds to a range in volume density of ~ 30–1000 cm^{-3} for the 0.3–1 kpc extent observed. This is considerably higher than is derived for direct bremsstrahlung (Table 6). The direct emission from such a plasma would thus dominate over the scattered flux unless the scattering medium had a temperature below $\sim 10^6$ K. In order not to absorb 1 keV X-rays, the scattering medium needs to be highly ionized. If this is achieved thermally then a temperature above $\sim 3 \times 10^6$ K is needed, in contradiction with the luminosity-derived temperature constraint above. In order to be self-consistent, then, the electron-scattering model requires the plasma to be photoionized at $\sim 10^5$ K some 1.5 kpc from the nucleus. To do this requires an ionization parameter close to $\Xi = 13$ (Krolik and Kallman 1984) for a power-law ionizing continuum of slope -1, since larger values (>33) give media that are too hot, and smaller values (<1) leave the medium opaque to soft X-rays (Krolik and Kallman 1984). To reach this level of ionization parameter using the central nuclear continuum requires luminosities of order 10^{47} ergs^{-1}, a factor of ~ 1000 larger than observed. Korista and Ferland (1989), however, find that for reasonable values a similar model can explain the extended emission in NGC 4151.

This hypothesis is open to direct tests. A scattered nuclear spectrum should share the same power-law X-ray spectrum (extending to tens of keV) as the nucleus. It should also have a scattered optical and ultraviolet component at the same fractional level. High spatial resolution X-ray spectra and sensitive optical polarization mapping would be tests of this possibility.

e) Outer Extended Region in NGC 1566

The approximately arcminute-scale structure in NGC 1566 (Fig. 3) may be a different phenomenon from the approximately arcsecond-scale emission in this and the other two Seyferts. The f_x/f_B ratio in this region is closer to that of normal spiral galaxies (Table 5; Fig. 3), so it may have a similar origin to their X-ray emission.

The large-scale X-ray excess is at p.a. $\sim 130°$. The minor axis of the whole galaxy, as determined from the outer region isophotes, is at p.a. 140° (Fig. 6; de Vaucouleurs 1973), and so there may be a relation with the X-ray emission. Minor axis outflows of X-ray hot gas have been seen in the starburst galaxies M82 (Watson, Stanger, and Griffiths 1984; Fabbiano 1988) and NGC 253 (Fabbiano 1988). Pence, Taylor, and Atherton (1990) have noted a region of peculiar [C III] velocities in this region covering a 90° long arc in the inner disk centered at p.a. 130°. The observed velocities are at $+60$ km s^{-1} with respect to the systemic velocity of the galaxy. The galaxy has an inclination of 27° to the plane of the sky so that this corresponds to a minor axis flow velocity of 67 km s^{-1}, too small to give keV X-rays if thermalized.

TABLE 7

COMPARISON OF STARBURST PLUMES WITH NGC 1566 ARCMINUTE-SCALE EMISSION

Galaxy	L_{Bol}(ergs s^{-1})	L_X(ergs s^{-1})	L_X/L_{Bol}
M82[a]	8×10^{43}	2×10^{39}	3×10^{-5}
NGC 253[a]	5×10^{43}	3×10^{39}	6×10^{-5}
NGC 1566	7×10^{43}[b]	$(9-12) \times 10^{40}$	1×10^{-3}

[a] Fabbiano 1988.
[b] Padovani 1989.

The nuclear bolometric (far-infrared to X-ray) luminosities of these starburst galaxies (M82 and NGC 253; Fabbiano 1988) are comparable, to within an order of magnitude, to that of NGC 1566 (Padovani 1989; Table 7). However, the total arcminute-scale X-ray luminosity of NGC 1566 is nearly 30–60 times larger than the X-ray luminosities of M82 and NGC 253 (Table 7) so that NGC 1566 would have to produce a nuclear outflow with much higher efficiency than the starburst galaxies.

The slightly bluer color of the outer region (Table 5) may suggest starburst activity. If the motions seen by Pence, Taylor, and Atherton are in the plane of the disk a velocity of 130 km s^{-1} would be implied, which might be related to such activity. It is not likely that the X-ray emission is associated with the bar seen at these radii since it lies at p.a. 354° (Fig. 6; de Vaucouleurs 1973). Indeed Hackwell and Schweizer (1983) have noted that, although the bar is prominent in the near infrared (*H* band), it is invisible in the ultraviolet (*U* band). A starburst in the bar is thus ruled out.

VI. CONCLUSIONS

There are now three cases of asymmetric, extended X-ray emission in Seyfert galaxies: NGC 1566, NGC 2992, and NGC 4151, out of five cases studied. Such extended regions of X-ray emission are thus quite common. These extended regions contain a significant fraction (15%–35%) of the X-ray luminosity of the nucleus in the HRI energy range. This emission can affect the interpretation of X-ray spectra in other AGN, particularly in similarly low-luminosity Seyferts.

With the limited resolution and signal-to-noise ratio of these maps, it is not possible to determine the cause of the extended X-ray emission. Nevertheless, nonthermal explanations—electron-scattered nuclear radiation (as is probably the case in NGC 1068), synchrotron or inverse Compton emission—seem less plausible than thermal models. These different possibilities are open to observational tests: X-ray spectra could tell us whether we are seeing hot gas, or an electron-scattered reflection of the nuclear spectrum. If a thermal bremsstrahlung model of the X-ray emission is relevant, then detailed maps of its morphology will be able to distinguish between radio jet–induced shock emission and a more diffuse medium in pressure balance with the optical emission-line gas and/or the radio lobes. Direct nonthermal synchrotron or inverse Compton emission from the radio jet could be distinguished by both spectral and morphological signatures.

Spatially resolved spectra will become possible only with *AXAF*, but higher resolution images with good signal-to-noise may be obtained with the HRI on *ROSAT*. Such observations are planned.

We thank G. Fabbiano and J. Halpern for valuable advice, S. Hazelton for assistance with making the X-ray maps, and K. Modestino for preparation of the manuscript. The SIMBAD data base was extremely useful for tracking down complete photometry for these galaxies, and we thank the SIMBAD staff for their efforts. This work was supported in part by NASA contract NAS8-30751 to the Smithsonian Astrophysical Observatory, and by NASA grants NAG8-462, NAG8-529, and NSF grant AST-8719207 to the University of Maryland.

REFERENCES

Antonucci, R. R., and Miller, J. S. 1985, *Ap. J.*, **297**, 621.
Avni, Y. 1976, *Ap. J.*, **210**, 642.
Bradt, H., and McClintock, J. 1983, *Ann. Rev. Astr. Ap.*, **21**, 13.
Branduardi-Raymont, G. 1986, in *The Physics of Accretion onto Compact Objects*, ed. K. O. Mason, M. G. Watson, and N. E. White (Berlin: Springer), p. 407.
Clements, E. D. 1981, *M.N.R.A.S.*, **197**, 829.
———. 1983, *M.N.R.A.S.*, **203**, 861.
Colina, L., *et al.* 1987, *Astr. Ap.*, **178**, 51.
Delvaille, J. P., Epstein, A., and Schnopper, H. W. 1978, *Ap. J.* (*Letters*), **219**, L81.
de Vaucouleurs, G. 1973, *Ap. J.*, **181**, 31.
de Vaucouleurs, G., de Vaucouleurs, A., and Corwin, H. G. 1976, *Second Reference Catalog of Bright Galaxies* (Austin: University of Texas).
Durret, F., and Bergeron, J. 1987, *Astr. Ap.*, **173**, 219.
Elvis, M., Briel, U., and Henry, J. P. 1983, *Ap. J.*, **268**, 105 (EBH).
Elvis, M., and Lawrence, A. 1988, *Ap. J.*, **333**, 161.
Elvis, M., Lockman, F. J., and Wilkes, B. J. 1989, *A.J.*, **97**, 777.
Fabbiano, G. 1988, *Ap. J.*, **330**, 672.
———. 1989, *Ann. Rev. Astr. Ap.*, **27**, 87.
Fabbiano, G., and Trinchieri, G. 1985, *Ap. J.*, **296**, 430.
Fabbiano, G., Trinchieri, G., and MacDonald 1984, *Ap. J.*, **284**, 65.
Fabian, A. C. 1977, *Nature*, **269**, 672.
Feigelson, E. D., Schreier, E. J., Delvaille, J. P., Giacconi, R., Grindlay, J. E., and Lightman, A. 1981, *Ap. J.*, **251**, 31.
Giacconi, R., *et al.* 1979, *Ap. J.*, **230**, 540.
Hackwell, J. A., and Schweizer, R. 1983, *Ap. J.*, **265**, 643.
Halpern, J. P. 1982, Ph.D. thesis, Harvard University.
———. 1985, *Ap. J.*, **290**, 130.
Harris, D. E., ed. 1984, *The Einstein Observatory Revised Users' Manual.*
Harris, D. E., Stern, C. P., and Biretta, J. A. 1990, in *Imaging X-Ray Astronomy*, ed. M. Elvis (Cambridge: Cambridge University Press), p. 299.
Harrison, B., Pedlar, A., Unger, S. W., Burgess, P., Graham, D. A., and Preuss, E. 1986, *M.N.R.A.S.*, **218**, 775.
Heckman, T. M., and Balick, B. 1983, *Ap. J.*, **268**, 102.
Heiles, C., and Cleary, M. N. 1979, *Australian J. Phys., Ap. Suppl.*, **47**, 1.
Henry, J. P., Kellogg, E. M., Briel, U. G., Murray, S. S., Van Speybroeck, L. P., and Bjorkholm, P. J. 1977, *Proc. Soc. Photo-Opt. Instrum. Eng.*, **106**, 196.
Hummel, E., van Gorkom, J. H., and Kotanyi, C. G. 1983, *Ap. J.* (*Letters*), **267**, L5.
Johnston, K. J., Elvis, M. Kjer, D., and Shen, B. S. P. 1982, *Ap. J.*, **262**, 61.
Korista, K. T., and Ferland, G. J. 1989, *Ap. J.* **343**, 678.
Koyama, K. 1989, in *IAU Symposium 134, Active Galactic Nuclei*, J. S. Miller and D. E. Osterbrock (Dordrecht: Reidel), p. 167.
Krolik, J. H., and Kallman, T. R. 1984, *Ap. J.*, **286**, 366.
Lawrence, A. 1980, *Ap. J.*, **192**, 83.
Longo, G., and de Vaucouleurs, A. 1983, *A General Catalogue of Photoelectric Magnitudes and Colors in the U, B, V System of 3,578 Galaxies Brighter than 16th Magnitude* (*1936–1982*) (Austin: University of Texas).
Maccacaro, T., Perola, G. C., and Elvis, M. 1982, *Ap. J.*, **257**, 47.
Manchester, R. N., and Taylor, J. H. 1981, *A.J.*, **86**, 1953.
Marshall, N., Warwick, R. S., and Pounds, K. A. 1981, *Ap. J.*, **194**, 987.
McAlary, C. W., McLaren, R. A., McGonegal, R. J., and Maza, J. 1983, *Ap. J. Suppl.*, **52**, 341.
Meurs, E. J. A., and Fosbury, R. A. E., eds. 1989, *Extranuclear Activity in Galaxies*, (Garching: ESO).
Neizvestny, S. I. 1986, *Soob. Spets. Astr. Obs.*, **51**, 5.
Padovani, P. 1989, *Astr. Ap.*, **209**, 27.
Pence, W. D., Taylor, K., and Atherton, P. *Ap. J.*, **357**, 415.
Penston, M. V., *et al.* 1990, preprint.
Pérez-Fournon, I., and Wilson, A. S. 1990, *Ap. J.*, **356**, 456.
Remillard, R. 1988, private communication.
Schreier, E. J., Gorenstein, P., and Feigelson, D. 1982, *Ap. J.*, **261**, 42.
Schulz, H. 1988, *Astr. Ap.*, **203**, 233.
Seward, F. D., and Martenis, P. 1986, *Catalog of Einstein* (*HEAO-2*) *Observations* (5th Ed.; SAO Special Report [CFA/HEA86-045]).
Simkin, S. M. 1975, *Ap. J.*, **200**, 567.
Stark, A. A., Heiles, C., Bally, J., and Linke, R. 1984, Bell Labs privately distributed magnetic tape.

Tucker, W. 1975, *Radiation Processes in Astrophysic* (Cambridge Mass.: MIT Press).
Turner, T. J., and Pounds, K. A. 1989, *M.N.R.A.S.*, **240**, 833.
Ulvestad, J. S., and Wilson, A. S. 1984, *Ap. J.*, **285**, 439.
Watson, M. G., Stanger, V., and Griffiths, R. E. 1984, *Ap. J.*, **286**, 144.
Wilson, A. S., and Heckman, T. M. 1985, in *Astrophysics of Active Galactic Nuclei and Quasi-Stellar Objects*, ed. J. S. Miller (Mill Valley, CA: University Science Books), p. 39.
Wilson, A. S., and Meurs, E. J. A. 1978, *Astr. Ap. Suppl.*, **33**, 107.
Wilson, A. S., and Ulvestad, J. S. 1982, *Ap. J.*, **263**, 576.
Yaqoob, T., Warwick, R. S., and Pounds, K. A. 1989, *M.N.R.A.S.*, **236**, 153.

U. Briel: Max-Planck-Institut für Extraterrestriche Physik, D8046 Garching, Federal Republic of Germany

M. Elvis and C. Fassnacht: Harvard-Smithsonian Center for Astrophysics, 60 Garden Street, Cambridge, MA 02138

A. S. Wilson: Astronomy Program, University of Maryland, College Park, MD 20742